BBA - Molecular Basis of Disease 1865 (2019) 98–106

Contents lists available at ScienceDirect

BBA - Molecular Basis of Disease

journal homepage: www.elsevier.com/locate/bbadis

Metabolomics of *Ndufs4*$^{-/-}$ skeletal muscle: Adaptive mechanisms converge at the ubiquinone-cycle

Karin Terburgh, Zander Lindeque, Shayne Mason, Francois van der Westhuizen, Roan Louw*

Human Metabolomics, Faculty of Natural and Agricultural Sciences, North-West University (Potchefstroom Campus), South Africa

ARTICLE INFO

Keywords:
Ndufs4 knockout mice
Skeletal muscle
Metabolomics
Mitochondrial disease
Complex I deficiency
Ubiquinone-cycle

ABSTRACT

Leigh syndrome is one of the most common childhood-onset neurometabolic disorders resulting from a primary oxidative phosphorylation dysfunction and affecting mostly brain tissues. *Ndufs4*$^{-/-}$ mice have been widely used to study the neurological responses in this syndrome, however the reason why these animals do not display strong muscle involvement remains elusive. We combined biochemical strategies and multi-platform metabolomics to gain insight into the metabolism of both glycolytic (white quadriceps) and oxidative (soleus) skeletal muscles from *Ndufs4*$^{-/-}$ mice. Enzyme assays confirmed severely reduced (80%) CI activity in both *Ndufs4*$^{-/-}$ muscle types, compared to WTs. No significant alterations were evident in other respiratory chain enzyme activities; however, *Ndufs4*$^{-/-}$ solei displayed moderate decreases in citrate synthase (12%) and CIII (18%) activities. Through hypothesis-generating metabolic profiling, we provide the first evidence of adaptive responses to CI dysfunction involving non-classical pathways fueling the ubiquinone (Q) cycle. We report a respective 48 and 34 discriminatory metabolites between *Ndufs4*$^{-/-}$ and WT white quadriceps and soleus muscles, among which the most prominent alterations indicate the involvement of the glycerol-3-phosphate shuttle, electron transfer flavoprotein system, CII, and proline cycle in fueling the Q cycle. By restoring the electron flux to CIII via the Q cycle, these adaptive mechanisms could maintain adequate oxidative ATP production, despite CI deficiency. Taken together, our results shed light on the underlying pathogenic mechanisms of CI dysfunction in skeletal muscle. Upon further investigation, these pathways could provide novel targets for therapeutic intervention in CI deficiency and potentially lead to the development of new treatment strategies.

1. Introduction

Mitochondria play a vital role in a myriad of processes involved in metabolism, cellular bioenergetics, and metabolic cell signaling [1–4]. The mitochondrial oxidative phosphorylation (OXPHOS) system, which comprises complexes I–IV and ATP synthase (CV), is the major contributor to cellular energy production and sustains most mitochondrial functions. The dysfunction of complex I (CI) (OMIM 252010) of the

Abbreviations: ^{1}H NMR, Proton nuclear magnetic resonance spectroscopy; 1-Mhis, 1-Methylhistidine; 2-AA, 2-Aminoadipate; 2-Mhis, 2-Methylhistidine; 5MTHF, 5-Methyl-tetrahydrofolate; Ala, Alanine; Arg, Arginine; Asn, Asparagine; Asp, Aspartate; BAIBA, β-Aminoisobutyrate; β-Ala, Beta-Alanine; C0, Carnitine; CI, complex I; C2, Acetyl-carnitine; CII, complex II; C3, Propionyl-carnitine; CIII, complex III; C4, Butyryl-carnitine; CIV, complex IV; C5, Isovalerylcarnitine; C6, Hexanoyl-carnitine; C8, Octanoyl-carnitine; C12, Dodecanoyl-carnitine; C14, Myristoyl-carnitine; C16, Palmitoyl-carnitine; C18, Stearoyl-carnitine; c-GPDH, Cytosolic glycerol-3-phosphate dehydrogenase; Cit, Citrulline; CS, Citrate synthase; Cyt c, Cytochrome c; DHAP, Dihydroxyacetone phosphate; DMG, N, *N*-Dimethylglycine; ETF, Electron transfer flavoprotein; ETF-QO, Electron transfer flavoprotein:ubiqionone oxidoreductase; FAD, Oxidized flavin adenine dinucleotide; $FADH_2$, Reduced flavin adenine dinucleotide; GC–TOF–MS, Gas chromatography time-of-flight mass spectrometry; GP, Glycerol-3-phosphate; Gln, Glutamine; Glu, Glutamate; Gly, Glycine; Hcys, Homocysteine; Hpro, Hydroxyproline; LC–MS/MS, Liquid chromatography tandem mass spectrometry; Lys, Lysine; Met, Methionine; m-FDH(s), Mitochondrial flavoprotein dehydrogenase(s); m-GPDH, Mitochondrial glycerol-3-phosphate dehydrogenase; NAA, *N*-Acetylaspartate; NAD^+, Oxidized nicotine amide adenine dinucleotide; NADH, Reduced nicotine amide adenine dinucleotide; NAG, *N*-Acetylglutamate; *Ndufs4*, NADH dehydrogenase (ubiquinone) iron-sulphur protein 4; *Ndufs4*$^{-/-}$, Homozygous *Ndufs4* knockout; Orn, Ornithine; OXPHOS, Oxidative phosphorylation; P-5-C, Pyrroline-5-carboxylate; pGlu, Pyroglutamate; Phe, Phenylalanine; Pip, Pipecolate; Pro, Proline; ProDH, Proline dehydrogenase; PYCR, Pyrroline-5-carboxylate reductase; Q, Ubiquinone (oxidized coenzyme Q10); QH_2, Ubiquinol (reduced coenzyme Q10); RC, Respiratory chain; SAH, *S*-Adenosylhomocysteine; SAM, *S*-Adenosylmethionine; Sar, Sarcosine; Ser, Serine; Tau, Taurine; THFA, Tetrahydrofolate; Thr, Threonine; TMG, Trimethylglycine; Tryp, Tryptophan; WT, Wild type (*Ndufs4*$^{+/+}$)

* Corresponding author at: Human Metabolomics, Faculty of Natural and Agricultural Sciences, North-West University (Potchefstroom Campus), Private Bag X6001, Potchefstroom, South Africa.

E-mail address: Roan.Louw@nwu.ac.za (R. Louw).

https://doi.org/10.1016/j.bbadis.2018.10.034
Received 4 September 2018; Received in revised form 23 October 2018; Accepted 29 October 2018
Available online 31 October 2018

OXPHOS system, is the most common defect in mitochondrial energy metabolism, often resulting in progressive, severe multi-system deterioration. Due to the extreme complexity and heterogeneous nature (genetically and clinically) of human CI deficiency, the underlying pathogenic mechanisms thereof remain poorly understood [5,6].

Current studies on mouse models of CI dysfunction, such as the whole-body *Ndufs4*$^{-/-}$ (knockout) mouse, attempt to better comprehend mitochondrial disease. The nuclear DNA-encoded NDUFS4 protein is essential to CI assembly, stability, and activity [7,8]. *Ndufs4*$^{-/-}$ mice present with symptoms similar to human CI deficiency at around postnatal day (P) 35 and develop a progressive Leigh-like phenotype, including developmental delays, failure to thrive, lethargy, ophthalmoplegia, locomotor impairment, hearing loss, as well as progressive ataxia, and necrotizing encephalomyopathy leading to early death (P50–60) [9–11]. Since the development of whole-body *Ndufs4*$^{-/-}$ mice, several conditional knockouts (neuronal, glial, cardiac, hematopoietic, and hepatic) have been developed in order to gain insight into tissue-specific consequences of CI dysfunction (reviewed by Toracco et al. [12]). However, due to the main interest in the predominant neurological phenotype of this disease model, limited information is available on skeletal muscle-specific consequences of the *Ndufs4* knockout.

A recent study by Foriel and colleagues [13] highlighted the involvement of skeletal muscle in *Ndufs4* knockout pathology. The authors reported similarities between the phenotypes of skeletal muscle-specific and whole-body *Ndufs4* knockout *Drosophila*, such as reduced lifespan, feeding difficulties, locomotor impairment, and climbing defects. Given the important, often underappreciated, role of the muscular system in health and disease [14], as well as its integration and interdependence with the nervous system [15], it is imperative to elucidate the effects of a *Ndufs4* knockout on muscle metabolism. Skeletal muscle not only facilitates breathing and locomotion but also plays an essential role in various systemic, energy-demanding processes such as whole-body protein metabolism, glucose, and fatty acid consumption, thermoregulation, immunity, as well as the maintenance of adequate bone strength and density [14–16]. As *Ndufs4*$^{-/-}$ mice display weight loss [9], a significant decrease in body fat [11], decreases in body temperature [9], as well as systemic inflammation and osteoporosis [10], it can be hypothesized that aberrant skeletal muscle metabolism might also play an important role in murine *Ndufs4*$^{-/-}$ phenotypes.

We aimed to gain insight into the consequences of a *Ndufs4*$^{-/-}$ on skeletal muscle bioenergetics and metabolism by combining biochemical strategies (respiratory chain enzyme assays) and multi-platform metabolic profiling (LC–MS/MS, GC–TOF–MS, and NMR analyses). Since the metabolic properties and subpopulations of muscle mitochondria depend on muscle fiber type composition [16], both glycolytic (white quadriceps; primarily type IIB myofibers) and oxidative (soleus; primarily type I myofibers) muscles were investigated. To the best of our knowledge, this is the first report of fiber type-specific enzymatic and metabolic data in *Ndufs4*$^{-/-}$ skeletal muscles. We report a metabolic signature consisting of 48 compounds in white quadriceps and 34 compounds in soleus muscles that distinguish whole-body *Ndufs4* knockout mice from wild types. These metabolic alterations provide insight into skeletal muscle-specific changes in metabolic pathways that result from whole-body mitochondrial dysfunction. These pathways could possibly be targeted in therapeutic interventions to promote muscle health in mitochondrial disorders and improve locomotion, metabolism, and quality of life.

2. Materials and methods

Detailed information regarding the described methods can be found in the supplementary data (Appendix A).

2.1. Animals and sampling

Male whole-body *Ndufs4* knockout mice (B6.129S4-*Ndufs4*$^{tm1.1Rpa}$/J; referred to as *Ndufs4*$^{-/-}$) along with age- and sex-matched controls (*Ndufs4*$^{+/+}$; referred to as WT) were used. *Ndufs4*$^{-/-}$ mice were born from heterozygous (*Ndufs4*$^{+/-}$) crosses obtained from Jackson Laboratory (ME, USA) (JAX stock #027058, https://www.jax.org/strain/027058). It should be noted that this mouse strain is BL6/J-derived and, therefore, potentially contains the *Nnt*$^{C57BL/6J}$ mutation. *Ndufs4* genotypes were confirmed by polymerase chain reaction (PCR) using tail snips. The animals were bred and housed at the specific pathogen-free (SPF) unit of the Vivarium (SAVC reg. no. FR15/13458) of the Pre-Clinical Drug Development Platform (PCDDP, NWU, RSA) and approval (NWU-00378-16-A5) for this study was obtained from the Animal Research Ethics Committee of the NWU. Animals were group housed under temperature- (22 ± 1 °C), humidity- (55 ± 10%) and light-controlled (12:12-h light/dark cycle) conditions with standard laboratory chow (Laboratory animal food: Rodent Breeder, Cat. #RM1845, LabChef, Nutritionhub) and water provided ad libitum. Mice were euthanized between postnatal day (P) 45–50 via cervical dislocation at the same time of day (8:00–9:00 AM) after overnight (12-h) fasting. From both hind limbs, white muscle portions of quadriceps femoris, as well as soleus muscles, were collected. Tissues were snap-frozen in liquid nitrogen (within 15 min *post-mortem*) and stored at −80 °C until used.

2.2. Enzyme assays

The enzyme activities of complex I (EC 1.6.5.3), complex II (EC 1.3.5.1), complex III (EC 1.10.2.2), and complex IV (EC 1.9.3.1) of the respiratory chain, as well as citrate synthase (EC 2.3.3.1), were measured in 700 × *g* supernatants of white quadriceps and soleus muscle homogenates. Analyses were performed on *Ndufs4*$^{-/-}$ (n = 12) and WT (n = 10) samples via standard operating procedures based on existing methods [17–19].

2.3. Metabolic profiling

Metabolic profiles were obtained from the white quadriceps and soleus muscles of *Ndufs4*$^{-/-}$ (n = 19) and WT (n = 20) mice using a multi-platform metabolomics approach. The analytical techniques were performed as previously described and comprised of targeted liquid chromatography-tandem mass spectrometry (LC–MS/MS) [20], untargeted gas chromatography time-of-flight mass spectrometry (GC–TOF–MS) [21], and proton nuclear magnetic resonance (^{1}H NMR) spectroscopy [22]. However, ^{1}H NMR spectroscopy could not be performed on soleus muscles, due to limited sample quantity. The data obtained in this study [23] can be accessed at the NIH Common Fund's Data Repository and Coordinating Center (supported by NIH grant, U01-DK097430) website, the Metabolomics Workbench, http://www.metabolomicsworkbench.org.

2.3.1. Extract preparation and derivatization

Muscle tissues were finely minced and homogenized in the presence of internal standards using a vibration mill. Metabolite extraction was achieved using a modified monophasic Bligh–Dyer extraction method [24] with a solvent ratio of 3:1:1 (methanol:water:chloroform). Details regarding the exact solvent volumes used for white quadriceps (~80 mg) and soleus (~5 mg) muscles can be found in the supplementary data (Appendix A). The water used for extraction contained a mixture of internal standards consisting of *N*, *N*-dimethyl-L-phenylalanine and 3phenylbutyric acid. Quality control (QC) samples were prepared from aliquots of all samples within a tissue type. Tissue extracts were divided into several vials (one for each analytical platform) and dried under nitrogen. Preparation per platform, in short, was: reconstitution in water for ^{1}H NMR; oximation and silylation for

GC–TOF–MS; as well as the addition of stable isotopes and butylation for LC–MS/MS.

2.4. Data processing

All data processing were done using Excel 2013 (Microsoft Inc.) and MetaboAnalyst 3.0 [25].

2.4.1. Enzyme assays

Enzyme activities were normalized to total protein (mg) content, reflecting tissue mass. Pretreatment of data involved generalized logarithm (glog) transformation.

2.4.2. Metabolic profiling

Spectral data obtained from the analytical platforms were extracted into matrices. Data matrices were individually inspected (correct peak picking and alignment, batch effect, and data integrity) as well as preprocessed (data filtering, missing value imputation, and normalization). Metabolites were normalized to tissue mass. This was achieved through normalization with either *N*, *N*-dimethyl-L-phenylalanine (GC–TOF–MS and LC–MS/MS data) or 3-phenylbutyric acid (^{1}H NMR data). In addition, metabolites measured with LC–MS/MS were further normalized to stable isotopes, which were added to samples before derivatization. Each metabolite was either normalized to its own isotope (where possible) or to an isotope with a similar retention time to which the metabolite strongly correlated. No batch corrections were needed as the QCs showed no significant batch effects. Thereafter, data pretreatment (glog transformation and mean centering) and outlier detection (principal component analysis (PCA) and heatmaps) were done.

2.5. Statistical analyses

2.5.1. Enzyme assays

Differences between *Ndufs4*$^{-/-}$ and WT enzyme activities were regarded as statistically significant with a Student's *t*-test p-value of < 0.05.

2.5.2. Metabolic profiling

Significantly discriminatory features between *Ndufs4*$^{-/-}$ and WT metabolic profiles were determined via univariate analyses. Statistically important differences (Student's *t*-test p-values) were inspected at a 5% and 10% significance level, and false discovery rate-adjusted p-values were calculated. The cut-off threshold for practical significance [26] was set at an effect size D-value of ≥ 0.5. The important features were visually investigated regarding their clustering, covariance, and discriminatory power via PCA as well as volcano plots. PCA was performed in MetaboAnalyst 3.0 [25] on a log-transformed and autoscaled dataset — comprising only the important metabolites identified on each platform. Finally, metabolite identities were assigned to spectral features, with high confidence levels [27,28]. Data set features were identified via spectral and retention time matching using commercial and in-house spectral libraries together with public databases.

3. Results and discussion

3.1. Respiratory chain enzyme activities in *Ndufs4*$^{-/-}$ muscles of different fiber type composition

The average (± SD) mitochondrial enzyme activities (respiratory chain complexes I-IV and citrate synthase) in *Ndufs4*$^{-/-}$ (n = 12) and WT (n = 10) white quadriceps and soleus muscles are summarized in Table 1. Enzyme activities were normalized to total protein (mg) content, rather than citrate synthase (CS) content, in order to focus on the relative enzyme capacity per tissue mass — thereby emphasizing the relative mitochondrial content of the two muscle fiber types, which was relevant to our metabolic results. In addition, Alam and colleagues [29] recently called into question whether CS activity could be considered a measure of mitochondrial volume in *Ndufs4*$^{-/-}$ mice. Through experimental and computational strategies, the authors reported significantly increased (72%) CS activity in *Ndufs4*$^{-/-}$ muscles — suggested to reflect an increase in Krebs cycle enzyme levels rather than mitochondrial content. With regard to our data, no significant difference in CS activity was found in *Ndufs4*$^{-/-}$ white quadriceps muscles compared to WTs; whereas a moderate decrease (12%, $p = 0.0149$) in CS activity was observed in *Ndufs4*$^{-/-}$ soleus muscles. Therefore, since a statistically significant difference was detected between WT and *Ndufs4*$^{-/-}$ soleus samples, normalization to CS would more than likely skew enzymatic data and lead to a distorted picture of the results. The lower *Ndufs4*$^{-/-}$ soleus CS activity we report, is in stark contrast to the 72% increase in CS activity previously reported for *Ndufs4*$^{-/-}$ (P35) hind limb muscles [29] — the difference could possibly be ascribed to the age difference between the mice studied or differences in the experimental procedures employed. However, several studies [9,30–32] on other *Ndufs4*$^{-/-}$ tissues have reported no alterations in CS activity, similar to the results we report here. This discrepancy should thus be investigated further.

Our data revealed a severe reduction (80%) in rotenone-sensitive CI activity ($p < 0.0001$) in both *Ndufs4*$^{-/-}$ white quadriceps and soleus muscles, compared to WTs. These results correspond with that reported for *Ndufs4*$^{-/-}$ skeletal muscle [7,29]. Although CI activity is reduced by the same factor in both muscles, glycolytic fibers have approximately 2–3 times fewer mitochondria than oxidative fibers [16]. Accordingly, with a *Ndufs4* knockout, our data demonstrate that glycolytic fibers display a much lower residual CI activity (4.58 ± 1.67 nmol/min/mg) than oxidative fibers (14.74 ± 6.67 nmol/min/mg). As evident from our metabolomics data (discussed in Section 3.4), this difference in residual CI activity reflects a biochemical threshold effect with the metabolic consequences of CI deficiency considerably more apparent in white quadriceps compared to soleus muscles. In agreement, model predictions by Alam and colleagues [29] (on entire hind limb *Ndufs4*$^{-/-}$ muscle) suggested that CI activity could be inhibited up to a critical value (90% of normal levels) before major metabolic consequences become apparent.

We found no significant differences in CII–CIV activities in *Ndufs4*$^{-/-}$ white quadriceps compared to WTs. However, in *Ndufs4*$^{-/-}$ soleus muscles, CIII activity was moderately decreased (18%, $p < 0.0001$). CIII has been shown to form a functional, albeit unstable, supercomplex with CI subassemblies in *Ndufs4*$^{-/-}$ muscle [7] and slight decreases in CIII activity have been reported in other tissues from *Ndufs4*$^{-/-}$ mice [9,31] as well as patients [30,33–36]. Literature reports on respiratory chain (RC) enzyme activities in *Ndufs4*$^{-/-}$ mice are quite diverse, with multiple studies [7,9,29–31] reporting variations in CII–CIV activity. This variation can possibly be attributed to tissue-specific differences, variances in sample preparation resulting in different amounts of functional enzyme (especially in the case of CI and supercomplexes thereof, due to its instability), as well as differences in the age of the mice at which point they were studied.

3.2. Statistical significance and discriminative power of *Ndufs4*$^{-/-}$ metabolic profiles

At 95% and 90% significance, univariate statistical analyses revealed a respective 48 (Table A.2) and 34 (Table A.3) discriminatory metabolites between *Ndufs4*$^{-/-}$ and WT white quadriceps and soleus muscles. Volcano plots (Fig. 1 A and B) depict the practical significance of all analytes detected by multi-platform metabolomics in white quadriceps and soleus muscles respectively. Significantly altered metabolites are indicated as decreased (green) or increased (red), while insignificant alterations are shown in gray. The five most decreased and increased metabolites are highlighted with ellipses and listed according to rank. As evident in the volcano plots, the majority of important

Table 1
Mitochondrial respiratory chain enzyme activities in skeletal muscles from WT and *Ndufs4*$^{-/-}$ mice.

Enzyme activity	White quadriceps			Soleus		
(nmol/min/mg)	WT	*Ndufs4*$^{-/-}$	*Ndufs4*$^{-/-}$/WT	WT	*Ndufs4*$^{-/-}$	*Ndufs4*$^{-/-}$/WT
CI	22.9 ± 5.9	4.58 ± 1.7*	0.20	81.2 ± 15.1	14.7 ± 6.7*	0.19
CII	29.9 ± 4.2	31.3 ± 5.0	1.05	63.1 ± 9.8	63.6 ± 10.3	1.01
CIII	430.2 ± 57.1	455.6 ± 47.8	1.06	1430.1 ± 105.1	1170.7 ± 97.4*	0.82
CIV	275.1 ± 32.4	273.8 ± 30.6	1.00	1033.1 ± 168.7	1077.0 ± 199.1	1.04
CS	233.4 ± 48.4	229.7 ± 50.6	0.98	636.7 ± 51.5	562.9 ± 75.3*	0.88

Enzyme activities normalized to mg protein. Average values (± SD) were obtained from 12 Ndufs4$^{-/-}$ and 10 WT animals. Significant differences in Ndufs4$^{-/-}$ enzyme activity relative to WTs are indicated with an asterisk (*$p < 0.05$). Abbreviations: CI, Complex I; CII, Complex II; CIII, Complex III; CIV, Complex IV; CS, Citrate synthase; WT, Wild type (Ndufs4$^{+/+}$).

metabolites were decreased in *Ndufs4*$^{-/-}$ muscles, compared to WTs, with the white quadriceps (Fig. 1A) displaying a more pronounced metabolic profile. The highest relative fold change was attributed to decreased levels of *N*, *N*-dimethylglycine (DMG), creatinine, and 2-aminoadipate (2AA), while the most prominent increases in metabolite levels (common to both muscles) were seen in lysine (Lys) and its catabolic product — pipecolate (Pip), as well as *N*-acetylaspartate (NAA). Multivariate PCA (Fig. 2) of significant metabolites revealed a partial separation in the clustering of *Ndufs4*$^{-/-}$ and WT groups in both muscles, indicating a distinct metabolic profile in *Ndufs4*$^{-/-}$ muscle.

3.3. Common metabolic alterations in *Ndufs4*$^{-/-}$ skeletal muscles of different fiber type composition

Numerous alterations in the levels of amino acids, acylcarnitines, and organic acids were evident in *Ndufs4*$^{-/-}$ skeletal muscles. The Venn diagram in Fig. 3 illustrates the number of similarities, as well as differences, observed between *Ndufs4*$^{-/-}$ metabolic profiles in the two muscles. Among the metabolites differing between genotypes, the majority (n = 26) were common to both white quadriceps and soleus muscles. Taken together, these adaptions revealed a similar bioenergetic flexibility in skeletal muscles of different fiber type composition. The most prominent changes in metabolite levels could be organized into several non-classical pathways involved in oxidative metabolism and redox regulation as depicted in Fig. 4. These pathways seem to participate in an attempt to increase (and restore) the electron flux to the RC via the ubiquinone (Q) pool, fueling CIII and allowing oxidative ATP production while bypassing CI in the process. A more in-depth discussion of the adaptive mechanisms involved in *Ndufs4*$^{-/-}$ skeletal muscle follows.

3.3.1. Glycolysis, triglyceride catabolism and the glycerol-3-phosphate (GP) shuttle

The accumulation of pyruvate and its derivatives, lactate, and alanine is considered a hallmark feature of mitochondrial metabolic dysfunction attributed to a disturbed redox balance (decreased NAD$^+$/NADH ratio) [37]. In agreement with this hallmark, Johnson and colleagues [11] reported the accumulation of pyruvate, lactate, and glycolytic intermediates in *Ndufs4*$^{-/-}$ whole-brain (P30). However, in *Ndufs4*$^{-/-}$ skeletal muscles, we observed significantly decreased levels of pyruvate, glycerol, and alanine along with significantly (white quadriceps) and moderately (soleus) decreased lactate levels. A possible mechanistic explanation for these observations is the activity of the glycerol-3-phosphate (GP) shuttle. Like lactate dehydrogenase, the GP shuttle rapidly re-oxidizes cytosolic NADH produced by glycolysis. However, an important difference between these redox regulatory mechanisms is the oxidative ATP producing capacity of the GP shuttle. Lying at the intersection of glycolysis, fatty acid metabolism, and oxidative phosphorylation, the GP shuttle serves as an alternative electron donor to the RC at the ubiquinone (Q) pool by transferring reducing equivalents from the cytosol to mitochondria. In this shuttle, the cytosolic enzyme, glycerol-3-phosphate dehydrogenase (c-GPDH, EC 1.1.1.8), oxidizes NADH to NAD$^+$ during the synthesis of GP from dihydroxyacetone phosphate (DHAP) — formed from either glycolysis or the phosphorylation of glycerol derived from triglyceride catabolism. GP can then be used as a substrate for the synthesis of either pyruvate, triglycerides, or phospholipids, however, in the case of the GP shuttle, GP is converted back to DHAP via the inner-membrane bound mitochondrial form of GPDH (m-GPDH) which reduces FAD to $FADH_2$. $FADH_2$ then reduces ubiquinone (Q) to ubiquinol (QH_2). The resulting DHAP is then recycled to again oxidize cytosolic NADH. Although understanding of the structure, function, and regulation of this system is still limited (reviewed by McDonald et al. [38]), several studies have suggested the important role of m-GPDH in thermogenesis and have shown it to be an important site of ROS production. Among the various metabolite shuttles responsible for the transfer of reducing equivalents from the cytosol to mitochondria, the GP shuttle is the most important in skeletal muscle [16]. Therefore, we postulate that the metabolic alterations we observed indicate the diversion of the glycolytic and triglyceride catabolic fluxes towards the GP shuttle in an attempt to not only restore the redox balance but also electron delivery to the RC at the Q pool. This mechanism could also possibly be involved in aberrant

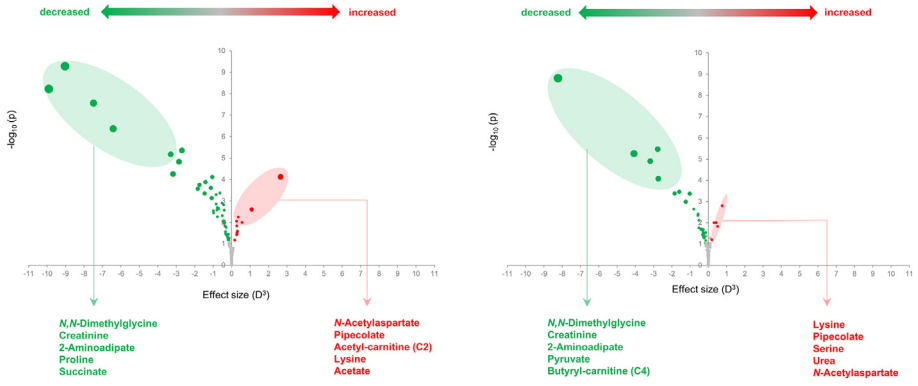

Fig. 1. Univariate analyses indicating the practical significance of important skeletal muscle metabolites. Volcano plots depicting multi-platform metabolomics results of A: white quadriceps muscles and B: soleus muscles from *Ndufs4*$^{-/-}$ mice (n = 19) compared to WTs (n = 20). The x-axis specifies the effect size raised to the third power (D^3) and the y-axis specifies the negative logarithm to the base 10 of the *t*-test p-values. Green and red symbols respectively indicate metabolites significantly lower or higher in *Ndufs4*$^{-/-}$ mice compared to WTs ($p < 0.1$ and $D \geq 0.5$). The five most significantly decreased and increased metabolites are highlighted and listed according to rank.

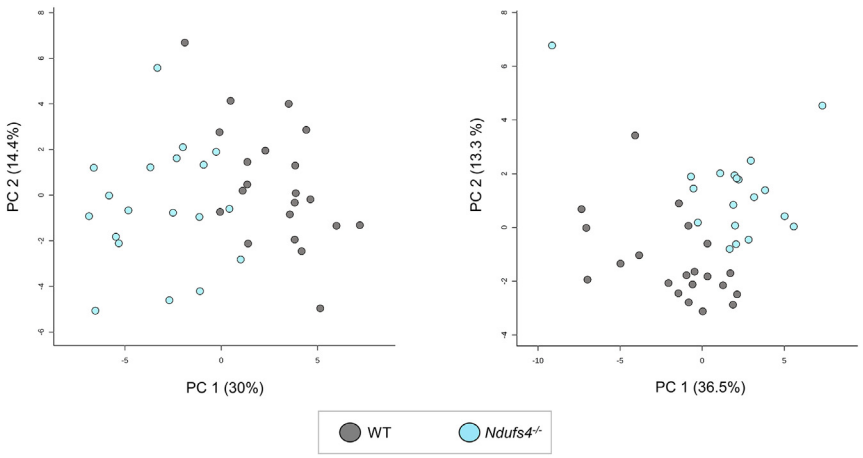

Fig. 2. Multivariate analyses indicating the discriminative power of important skeletal muscle metabolites. Principal component analysis (PCA) scores plots depicting significant metabolites ($p < 0.1$, $D \geq 0.5$) identified in A: white quadriceps muscles and B: soleus muscles. Partial separation in the clustering of *Ndufs4*$^{-/-}$ (n = 19, blue) and WT (n = 20, gray) groups are visible in both cases. White quadriceps: PC1 and PC2 account for 30.0% and 14.4% of variation respectively. Soleus: PC1 and PC2 account for 36.5% and 13.3% of variation respectively.

ROS production, a feature often reported in mitochondrial disease.

3.3.2. β-oxidation, amino acid catabolism, and the electron transfer flavoprotein (ETF/ETF-QO) system

Both *Ndufs4*$^{-/-}$ skeletal muscle types displayed dramatic decreases in the levels of *N*, *N*-dimethylglycine (DMG), fatty acid acylcarnitines of even (C0, C4, C6, C8, C12, and C16) and odd (C3 and C5) chain length, as well as 2-aminoadipate (2-AA). Although previous metabolomics investigations on mitochondrial disease have reported disturbances in one-carbon metabolism, the catabolism of fatty acids, branched-chain amino acids (BCAA), as well as the ketogenic amino acid, lysine, the underlying mechanisms remain unclear [37]. We postulate that these diverse metabolic alterations point to several pathways that converge at the electron transfer flavoprotein (ETF/ETF-QO) system. The ETF/ETF-QO system functions as an electron transfer pathway conducting electrons from eleven mitochondrial flavoprotein dehydrogenases (m-FDHs) to the Q pool of the RC. These m-FDHs include enzymes involved in mitochondrial one-carbon metabolism (dimethylglycine dehydrogenase, EC 1.5.99.2; and sarcosine dehydrogenase, EC 1.5.99.1), fatty acid β-oxidation (short-chain acyl-CoA dehydrogenase, EC 1.3.99.2; medium-chain acyl-CoA dehydrogenase, EC 1.3.99.3; and long-chain acyl-CoA dehydrogenase, EC 1.3.99.13), as well as branched-chain amino acid catabolism (isovaleryl-CoA dehydrogenase, EC 1.3.99.10; and isobutyryl-CoA dehydrogenase) and lysine catabolism (glutaryl-CoA dehydrogenase, EC 1.3.99.7) (reviewed by Watmough et al. [39]). Therefore we hypothesize that, in *Ndufs4*$^{-/-}$ skeletal muscle, there is an increased flux through these m-FDHs supplying the ETF/ETF-QO system with electrons in order to compensate for decreased electron transfer from CI. This increased flux, in part, could lead to the observed decreased metabolite levels. However, this switch in flux cannot effectively compensate for the CI defect as all of these $FADH_2$ producing pathways also require NAD^+ as a co-factor. NADH levels could build up due to CI inactivity as well as these compensatory reactions themselves. The hypothesized result of the altered redox state and shortage of NAD^+ is seen in the lysine catabolic pathway. Lysine is normally catabolized to 2AA via the saccharopine pathway, which requires $NADP^+$ and two NAD^+ molecules. The subsequent conversion of 2-AA to glutaryl-CoA (substrate for ETF/ETF-QO system) requires an additional NAD^+ molecule. In addition to decreased 2-AA levels, we observed the accumulation of lysine and its alternative catabolite, pipecolate (Pip), in *Ndufs4*$^{-/-}$ skeletal muscles — indicating that an alternative non-NAD^+-consuming catabolic route is preferred, resulting in an even larger reduction in 2-AA levels. Altogether, the data suggest that βoxidation and amino acid catabolism might fuel the Q cycle via the ETF/ETF-QO system, even though a disturbed redox balance might limit the efficacy of some of the reactions.

When comparing previous metabolomics studies on *Ndufs4* knockout mice with our current observations, similar ambiguous effects on lipid metabolism are noticeable. In *Ndufs4*$^{-/-}$ liver, markedly reduced levels of fat droplets and free fatty acids were reported [11];

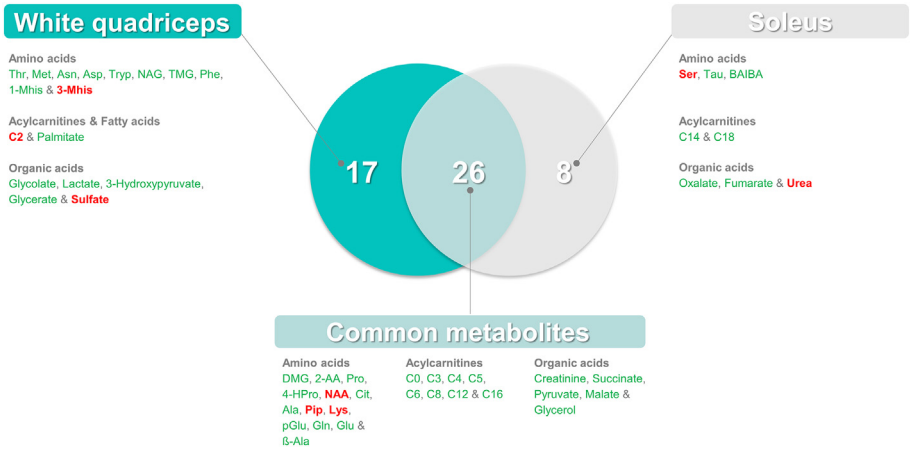

Fig. 3. Venn diagram of important metabolites discriminating *Ndufs4*$^{-/-}$ and WT groups in skeletal muscles. Green and red respectively indicate metabolites significantly ($p < 0.1$ and $D \geq 0.5$) lower or higher in *Ndufs4*$^{-/-}$ mice (n = 19) compared to WTs (n = 20). Among the important metabolites identified, 26 were common to both muscles, while several alterations were unique to the quadriceps (n = 17) and soleus (n = 8). Important metabolites (n = 5) identified in white quadriceps muscles by NMR spectroscopy were excluded from the comparison as soleus samples were not analyzed on that analytical platform due to limited sample quantity. Abbreviations: 1-Mhis, 1-Methylhistidine; 2-AA, 2-Aminoadipate; 2-Mhis, 2-Methylhistidine; Ala, Alanine; Asn, Asparagine; Asp, Aspartate; BAIBA, β-aminoisobutyrate; β-Ala, Beta-alanine; C0, Carnitine; C2, Acetyl-carnitine; C3, Propionyl-carnitine; C4, Butyryl-carnitine; C5, Isovaleryl-carnitine; C6, Hexanoyl-carnitine; C8, Octanoyl-carnitine; C12, Dodecanoyl-carnitine; C14, Myristoyl-carnitine; C16, Palmitoyl-carnitine; C18, Stearoyl-carnitine; Cit, Citrulline; DMG, N, *N*-Dimethylglycine; Gln; Glutamine; Glu, Glutamate; Hpro, Hydroxyproline; Lys, Lysine; Met, Methionine; NAA, N-Acetylaspartate; NAG, N-Acetylglutamate; pGlu, Pyroglutamate; Phe, Phenylalanine; Pip, Pipecolate; Pro, Proline; Ser, Serine; Tau, Taurine, Thr, Threonine; TMG, Trimethylglycine; Tryp, Tryptophan.

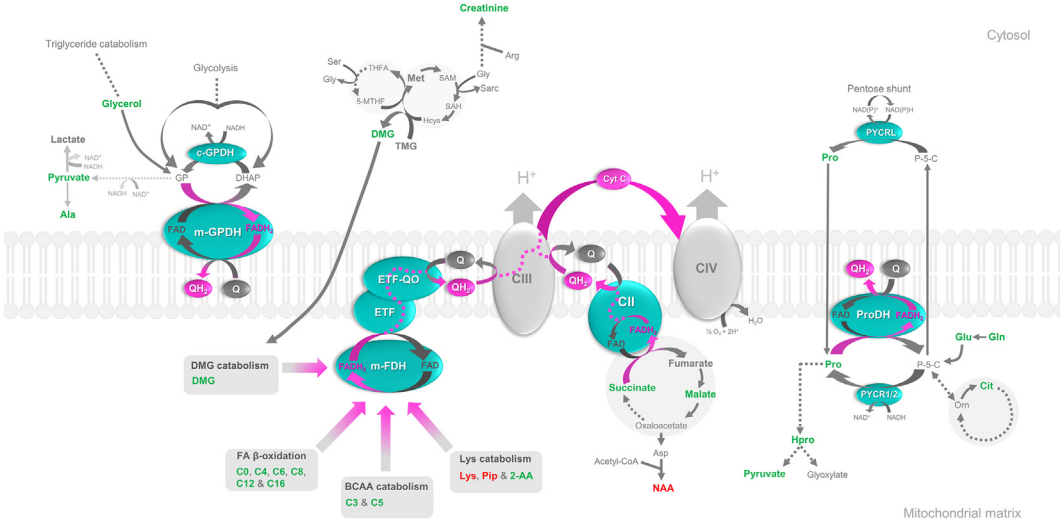

Fig. 4. Common metabolic alterations in *Ndufs4*$^{-/-}$ skeletal muscles. *Ndufs4*$^{-/-}$ quadriceps and soleus skeletal muscles both show a metabolic shift towards several non-classical pathways involved in oxidative metabolism and redox regulation, in an attempt to restore electron delivery to the respiratory chain via the ubiquinone (Q) pool. Green and red indicate metabolite levels significantly lower or higher, respectively, in *Ndufs4*$^{-/-}$ mice (n = 19) compared to WTs (n = 20). Pink arrows indicate electron flow. Dashed lines reflect multi-step reactions not fully shown. Multi-platform metabolic profiling of *Ndufs4*$^{-/-}$ skeletal muscles indicates (from left to right): 1) a shift in glycolysis and triglyceride catabolism towards the glycerol-3-phosphate shuttle, which re-oxidizes cytosolic NADH while serving as an electron donor to the respiratory chain via the mitochondrial enzyme glycerol-3-phosphate dehydrogenase (m-GPDH); 2) a shift in flux through several mitochondrial flavoprotein dehydrogenases (m-FDH) involved in one-carbon metabolism (dimethylglycine dehydrogenase), fatty acid β-oxidation (short-, medium- and long-chain acyl-CoA dehydrogenase), and amino acid catabolism (isobutyryl-, isovaleryl- and glutaryl-CoA dehydrogenase) which supply electrons to the respiratory chain via the electron transfer flavoprotein (ETF/ETF-QO) system; 3) a shift in flux through the Krebs cycle to increase electron delivery to the respiratory chain via complex II (CII; succinate dehydrogenase); and 4) increased mitochondrial cycling of proline and pyrroline-5-carboxylate (P-5-C) to directly provide electrons to the respiratory chain via proline dehydrogenase and sustain NAD^+ levels. Abbreviations: Enzymes in blue: ETF, Electron transfer flavoprotein; ETF-QO, Electron transfer flavoprotein:ubiquinone oxidoreductase; m-FDH(s), Mitochondrial flavoprotein dehydrogenase(s); m-GPDH, Mitochondrial glycerol-3-phosphate dehydrogenase; c-GPDH, Cytosolic glycerol-3-phosphate dehydrogenase; CII, Complex II or succinate dehydrogenase; ProDH, Proline dehydrogenase; PYCR, Pyrroline-5-carboxylate reductase; Cyt c, Cytochrome c. Electron carriers: FAD, Oxidized flavin adenine dinucleotide; $FADH_2$, Reduced flavin adenine dinucleotide; NAD^+, Oxidized nicotine amide adenine dinucleotide; NADH, Reduced nicotine amide adenine dinucleotide; Q, Ubiquinone (oxidized coenzyme Q); QH_2, Ubiquinol (reduced coenzyme Q). Metabolites: 2-AA, 2-Aminoadipate; 5-MTHF, 5-Methyltetrahydrofolate; Ala, Alanine; Arg, Arginine; Asp, Aspartate; C0, Carnitine; C12, Dodecanoyl-carnitine; C16, Palmitoyl-carnitine; C3, Propionyl-carnitine; C4, Butyryl-carnitine; C5, Isovaleryl-carnitine; C6, Hexanoyl-carnitine; C8, Octanoyl-carnitine; Cit, Citrulline; DHAP, Dihydroxyacetone phosphate; DMG, *N*, *N*-Dimethylglycine; GP, Glycerol-3-phosphate; Gln; Glutamine; Glu, Glutamate; Gly, Glycine; Hcys, Homocysteine; Hpro, Hydroxyproline; Lys, Lysine; Met, Methionine; NAA, N-Acetylaspartate; Orn, Ornithine; P-5-C, Pyrroline-5-carboxylate; Pip, Pipecolate; Pro, Proline; SAH, S-adenosylhomocysteine; SAM, S-adenosylmethionine; Sar, Sarcosine; Ser, Serine; THFA, Tetrahydrofolate.

while significantly increased blood hydroxy-acylcarnitine (C4:0, C16:0, and C18:1) levels were reported in a comparable *Ndufs4* knockout mouse model (*Ndufs4*$^{fky/fky}$) [32]. The latter observation was postulated to reflect a blockage in the NAD^+-dependent (third) step of βoxidation. However, upon further investigation, *Ndufs4*$^{fky/fky}$ liver and heart revealed no alterations in carnitine species, while skeletal muscle displayed no detectable lipid accumulation via Oil Red O staining [32]. These observations could fit into our combined hypotheses of decreased lipogenesis and increased lipolysis due to the activity of the GP shuttle, as well as increased fatty acid βoxidation, albeit inefficient due to a redox imbalance.

3.3.3. One-carbon metabolism, the methylation cycle, and the transsulfuration pathway

The altered redox state, as well as the postulated use of DMG by the ETF/ETF-QO system, seem to contribute to the disruption of one-carbon metabolism, the methylation cycle, and the transsulfuration pathway. These disturbances were more prominent in white quadriceps muscles which, along with decreased levels of DMG, displayed significantly decreased levels of trimethylglycine (betaine), methionine, threonine, and the accumulation of choline. Trimethylglycine (TMG) originates from the NAD^+ dependent catabolism of choline, which takes place in mitochondria. DMG is then produced from TMG in a folate-independent cytosolic reaction during which homocysteine is re-methylated to methionine. NAD^+ shortage could, therefore, cause choline build up and a further reduction in DMG levels. As DMG also has the ability to yield one-carbon units via folate-dependent mitochondrial reactions involving dimethylglycine dehydrogenase (which produces sarcosine) and sarcosine dehydrogenase (which produces glycine), this metabolite links one-carbon metabolism to the ETF/ETF-QO system.

Furthermore, in both *Ndufs4*$^{-/-}$ skeletal muscle types, dramatic decreases were seen in creatinine levels along with slightly (not significantly) reduced creatine levels. Creatine biosynthesis takes place chiefly in the liver and kidneys, however, a small amount of skeletal muscle creatine stores have been shown to be produced in the muscles themselves [40]. Creatine biosynthesis is a two-step reaction involving the conversion of arginine and glycine to guanidinoacetate, which is then methylated via SAM to form creatine and SAH. A disturbance in one-carbon metabolism could lead to lowered SAM available for methylation reactions, therefore dramatic decreases in creatinine could reflect the disrupted methylation of guanidinoacetate to creatine. In agreement, significantly reduced levels of 1-methylhistidine (1-Mhis) and increased levels of histamine in *Ndufs4*$^{-/-}$ white quadriceps could also reflect disturbed methylation reactions. On the whole, the observed metabolic alterations indicate disturbances in one-carbon metabolism and methylation reactions, possibly due to a disturbed redox balance and derangements in DMG metabolism.

3.3.4. The Krebs cycle and mitochondrial complex II (succinate dehydrogenase)

We observed significantly decreased levels of succinate and malate in both muscles along with significant (soleus) and moderate (white quadriceps) reductions in fumarate levels. A similar observation was made in *Ndufs4*$^{-/-}$ (P35) hind limb skeletal muscle by Alam and

colleagues [29], who reported decreased succinate levels along with an increase in flux (10–11%) through reactions providing substrates to CII and a slight decrease in the other (generally NAD^+ consuming) reactions which mainly fuel CI. The reduction in metabolite levels we observed could, therefore, reflect an increased use of succinate to fuel CII and the respiratory chain via the Q pool together with a decreased resupply thereof due to a congested Krebs cycle. In addition, we observed increased levels of *N*-acetylasparte (NAA) which is hypothesized to be an alternative storage and transport form of acetate and has been suggested to play a role in lipid metabolism and posttranslational protein modification [41]. Although the physiological functions of NAA are still poorly understood, it was recently discovered that NAA metabolism is not exclusive to the brain as previously thought. Aberrant NAA metabolism has been reported in mitochondrial disease, however, to the best of our knowledge this is the first report thereof in skeletal muscle. NAA is synthesized from aspartate and acetyl-CoA by aspartate *N*-acetyltransferase (Asp-NAT, EC 2.3.1.17). In skeletal muscle, the expression of *Nat8l* mRNA (encoding Asp-NAT) has been observed, although levels were reported to be negligible [41]. We, therefore, hypothesize that the rate of acetyl-CoA synthesis from sources like β-oxidation and lysine catabolism (which fuel the ETF/ETF-QO system) exceeds the rate at which the Krebs cycle can utilize the molecule, therefore acetyl-CoA accumulates and is converted to NAA [41].

3.3.5. Proline metabolism and the proline cycle

Although there is still much to be learned about the precise mechanism and functions of the proline cycle, the vital role of this relatively novel pathway in health and disease is becoming increasingly clear (reviewed by Phang et al. [42]). Some of the most striking metabolic alterations we observed in *Ndufs4*$^{-/-}$ skeletal muscles included the reduction of proline, hydroxyproline (Hpro), citrulline, glutamate, and glutamine levels. These alterations could reflect aberrant proline metabolism, which is strongly associated with the pentose phosphate pathway, urea cycle, and Krebs cycle. The mitochondrial flavin-dependent enzyme, proline dehydrogenase (ProDH, EC 1.5.99.8), together with the cytosolic (PYCRL) and mitochondrial (PYCR1/2) isoforms of pyrroline-5-carboxylate reductase (EC 1.5.1.2) are responsible for the interconversions of proline and pyrroline-5-carboxylate (P-5-C) constituting the proline cycle. Proline can directly act as an alternative source of electron delivery to the RC Q pool, through its catabolism to P-5-C via ProDH. P-5-C can also be synthesized from either glutamate or ornithine while its conversion back to proline regenerates $NAD(P)^+$. We, therefore, postulate that the adaptive increased cycling of proline and P-5-C might serve to sustain QH_2 and $NAD(P)^+$ levels. In addition to energy production and redox homeostasis, proline metabolism has been shown to be involved in ROS production, the initiation of apoptosis, autophagy, as well as protein and nucleotide synthesis while proline's post-translational product, hydroxyproline, has recently been recognized as a substrate for the synthesis of pyruvate, glucose, and glycine (reviewed by Wu et al. [43]). Taken together, proline metabolism might play a central role in several metabolic pathway derangements often reported in mitochondrial disease.

3.4. Fiber type-specific metabolic alterations in Ndusf4$^{-/-}$ skeletal muscles

When looking at the difference between the important metabolites identified in *Ndufs4*$^{-/-}$ muscles (Fig. 3), seventeen metabolites were uniquely altered in the white quadriceps while eight alterations were unique to the soleus. This comparison excludes the five important metabolites detected with NMR spectroscopy as soleus samples were not analyzed on that analytical platform due to limited sample quantity. Altogether, glycolytic fibers (white quadriceps) seemed to show more pronounced metabolic disturbances in response to CI deficiency with NAA accumulation being more than two-fold higher than in soleus muscles, along with an additional accumulation of acetyl-CoA derivatives, acetate, and acetyl-carnitine (C2). In addition, *Ndufs4*$^{-/-}$ white quadriceps muscles showed significant 3-methylhistidine accumulation, which is indicative of myofibrillar protein breakdown [44]. This observation agrees with literature reports of glycolytic fibers showing more pronounced atrophy than oxidative fibers in pathological conditions affecting muscle protein balance, and aging [16]. Taken together with the greater disturbance in methylation reactions we observed in white quadriceps muscles (discussed in Section 3.3.3), these alterations could indicate more profound disruptions of the redox balance (NAD^+/NADH ratio), Krebs cycle congestion and possible acetyl-CoA accumulation in more glycolytic muscle fibers. In addition to less dramatic metabolic alterations than in the white quadriceps, we saw significantly increased levels of serine along with decreased levels of taurine and pyroglutamate in *Ndufs4*$^{-/-}$ soleus muscles. These alterations could indicate a shift in glycolysis towards serine production, which could be used for glutathione synthesis — a phenomenon often described in mitochondrial disease due to increased electron leak and ROS production. As oxidative fibers have been shown to have a greater supply of substrates, oxygen, and more mitochondria (with greater oxidative capacity) [16], it can be postulated that mitochondrial ROS levels — due to the CI deficiency — are higher in *Ndufs4*$^{-/-}$ soleus muscles and therefore the need for glutathione ROS scavenging is greater. Furthermore, our results suggest that BCAA catabolism might be more dramatically affected in soleus muscles as we observed moderately (but not significantly) increased levels of valine and leucine, significant decreases in β-aminoisobutyrate (BAIBA) levels, and much greater decreases in C5- and C3-carnitine levels than in the white quadriceps muscles. Hence, the data could point to a more effectively functioning Krebs cycle and a better metabolic adaption of soleus muscles to the CI defect.

4. Conclusions

We report the first fiber type-specific enzymatic and metabolic data in *Ndufs4*$^{-/-}$ skeletal muscles. Enzyme assays revealed a severe reduction (80%) in CI activity in both glycolytic (white quadriceps) and oxidative (soleus) muscles from whole-body *Ndufs4*$^{-/-}$ mice. Such an extreme reduction in CI activity would greatly reduce the electron flux to the rest of the respiratory chain (RC). As an adaptive response in both tissues, our metabolic data suggest that alternative fuels and non-classical pathways serve to sustain the RC ubiquinol (QH_2) pool, thereby restoring electron flux to CIII through the ubiquinone (Q) cycle. However, despite these metabolic adaptions in skeletal muscle, a disturbed redox balance still seems to result in congested mitochondrial pathways. Metabolic and bioenergetic disturbances due to CI deficiency seem to be more evident in glycolytic fibers, possibly due to their innately lower mitochondrial content. Some of the most significant metabolic alterations we observed in *Ndufs4*$^{-/-}$ muscles implicate the involvement of the glycerol-3-phosphate (GP) shuttle, the electron transfer flavoprotein (ETF/ETF-QO) system, complex II of the RC, and the proline cycle in electron delivery to the Q pool. Some of these mechanisms might also serve to restore NAD^+ levels (GP shuttle and proline cycle), while others could contribute to redox imbalance (NAD^+ consuming reactions fueling ETF/ETF-QO and the Krebs cycle) in CI deficiency. Altogether, the observed adaptive mechanisms could explain the apparent lack of an obvious muscle phenotype in *Ndufs4*$^{-/-}$ mice, as well as the reported ability of skeletal muscle to maintain normal ATP production, despite CI deficiency [9,29]. However, the hypotheses generated in this study need to be followed up/validated in more targeted metabolic studies on *Ndufs4*$^{-/-}$ mice. For now, it remains unclear whether these adaptive responses are capable of sustaining energy homeostasis when challenged with exercise or nutrient deprivation. A comparison of these and related metabolic pathways in other tissues (e.g. the brain) could possibly provide answers to tissue-specific phenotypes and novel insight in targeted therapeutic interventions.

Transparency document

The Transparency document associated with this article can be found, in online version.

Acknowledgments

Funding: This work was supported by the National Research Foundation of South Africa (NRF; Grant numbers 92736 and 111247) and the Technological Innovation Agency of the Department of Science and Technology, Republic of South Africa (TIA; Grant number Metabol. 01). Opinions expressed and conclusions arrived at, are those of the authors and are not necessarily to be attributed to the NRF or the TIA. We thank Kobus Venter and Antoinette Fick from the Pre-Clinical Drug Development Platform (PCDDP, NWU, RSA), for their assistance regarding animal handling.

Conflict of interest

All authors declare that they have no conflict of interest.

Ethical approval

The AnimCare animal research ethics committee of North-West University approved (NWU-00378-16-A5) the animal protocols used in this study. All animals were maintained and all procedures performed in accordance with the code of ethics in research, training, and testing of drugs in South Africa and complied with national legislation.

Appendix A. Supplementary data

Supplementary data to this article can be found online at https://doi.org/10.1016/j.bbadis.2018.10.034.

References

[1] D.T. Shaughnessy, K. McAllister, L. Worth, A.C. Haugen, J.N. Meyer, F.E. Domann, B. Van Houten, R. Mostoslavsky, S.J. Bultman, A.A. Baccarelli, T.J. Begley, R.W. Sobol, M.D. Hirschey, T. Ideker, J.H. Santos, W.C. Copeland, R.R. Tice, D.M. Balshaw, Mitochondria, energetics, epigenetics, and cellular responses to stress, Environ. Health Perspect. 122 (2014) 1271–1278.
[2] I.N. Shokolenko, M.F. Alexeyev, Mitochondrial DNA: a disposable genome? Biochim. Biophys. Acta 1852 (2015) 1805–1809.
[3] L.C. Greaves, A.K. Reeve, R.W. Taylor, D.M. Turnbull, Mitochondrial DNA and disease, J. Pathol. 226 (2012) 274–286.
[4] A.D. Cherry, C.A. Piantadosi, Regulation of mitochondrial biogenesis and its intersection with inflammatory responses, Antioxid. Redox Signal. 22 (2015) 965–976.
[5] E. Fassone, S. Rahman, Complex I deficiency: clinical features, biochemistry and molecular genetics, J. Med. Genet. 49 (2012) 578–590.
[6] F. Distelmaier, W.J.H. Koopman, L.P. van den Heuvel, R.J. Rodenburg, E. Mayatepek, P.H.G.M. Willems, J.A.M. Smeitink, Mitochondrial complex I deficiency: from organelle dysfunction to clinical disease, Brain 132 (2009) 833–842.
[7] M.A. Calvaruso, P. Willems, M. van den Brand, F. Valsecchi, S. Kruse, R. Palmiter, J. Smeitink, L. Nijtmans, Mitochondrial complex III stabilizes complex I in the absence of NDUFS4 to provide partial activity, Hum. Mol. Genet. 21 (2012) 115–120.
[8] F. Valsecchi, W.J.H. Koopman, G.R. Manjeri, R.J. Rodenburg, J.A.M. Smeitink, P.H.G.M. Willems, Complex I disorders: causes, mechanisms, and development of treatment strategies at the cellular level, Dev. Disabil. Res. Rev. 16 (2010) 175–182.
[9] S.E. Kruse, W.C. Watt, D.J. Marcinek, R.P. Kapur, K.A. Schenkman, R.D. Palmiter, Mice with mitochondrial complex I deficiency develop a fatal encephalomyopathy, Cell Metab. 7 (2008) 312–320.
[10] Z. Jin, W. Wei, M. Yang, Y. Du, Y. Wan, Mitochondrial complex I activity suppresses inflammation and enhances bone resorption by shifting macrophage-osteoclast polarization, Cell Metab. 20 (2014) 483–498.
[11] S.C. Johnson, M.E. Yanos, E.–.B. Kayser, A. Quintana, M. Sangesland, A. Castanza, L. Uhde, J. Hui, V.Z. Wall, A. Gagnidze, K. Oh, B.M. Wasko, F.J. Ramos, R.D. Palmiter, P.S. Rabinovitch, P.G. Morgan, M.M. Sedensky, M. Kaeberlein, mTOR inhibition alleviates mitochondrial disease in a mouse model of Leigh syndrome, Science 342 (2013) 1524–1528.
[12] A. Torraco, S. Peralta, L. Iommarini, F. Diaz, Mitochondrial diseases part I: mouse models of OXPHOS deficiencies caused by defects on respiratory complex subunits or assembly factors, Mitochondrion (2015) 76–91.
[13] S. Foriel, J. Beyrath, I. Eidhof, R.J. Rodenburg, A. Schenck, J.A.M. Smeitink, Feeding difficulties, a key feature of the *Drosophila* NDUFS4 mitochondrial disease model, Dis. Model. Mech. 11 (2018).
[14] R.R. Wolfe, The underappreciated role of muscle in health and disease, Am. J. Clin. Nutr. 84 (2006) 475–482.
[15] M.F. Goody, C.A. Henry, A need for NAD^+ in muscle development, homeostasis, and aging, Skelet. Muscle 8 (2018) 9.
[16] S. Schiaffino, C. Reggiani, Fiber types in mammalian skeletal muscles, Physiol. Rev. 91 (2011) 1447–1531.
[17] D. Shepherd, P.B. Garland, The kinetic properties of citrate synthase from rat liver mitochondria, Biochem. J. 114 (1969) 597–610.
[18] A.J.M. Janssen, F.J.M. Trijbels, R.C.A. Sengers, J.A.M. Smeitink, L.P. van den Heuvel, L.T.M. Wintjes, B.J.M. Stoltenborg–Hogenkamp, R.J.T. Rodenburg, Spectrophotometric assay for complex I of the respiratory chain in tissue samples and cultured fibroblasts, Clin. Chem. 53 (2007) 729–734.
[19] S. Rahman, R.B. Blok, I.H.-H.M. Dah, D.M. Danks, D.M. Kirby, C.W. Chow, J. Christodoulou, D.R. Thorburn, Leigh syndrome: clinical features and biochemical and DNA abnormalities, Ann. Neurol. 39 (1996) 343–351.
[20] C.M.C. Mels, P. Jansen Van Rensburg, F.H. van der Westhuizen, P.J. Pretorius, E. Erasmus, Increased excretion of C4–carnitine species after a therapeutic acetylsalicylic acid dose: evidence for an inhibitory effect on short–chain fatty acid metabolism, ISRN Pharmacol. 2011 (2011) 851870.
[21] J.Z. Lindeque, J. Hidalgo, R. Louw, F.H. van der Westhuizen, Systemic and organ specific metabolic differences in metallothionein knockout mice when challenged with exercise, Metabolomics 9 (2013) 418–432.
[22] S.W. Mason, K. Terburgh, R. Louw, Miniaturized ^{1}H–NMR method for analyzing limited–quantity samples applied to a mouse model of Leigh disease, Metabolomics 14 (2018) 74.
[23] K. Terburgh, J.Z. Lindeque, S.W. Mason, F.H. Van der Westhuizen, R. Louw, Multi-platform metabolomics data from Ndufs4$^{-/-}$ skeletal muscles, Metabolomics Workbench, http://www.metabolomicsworkbench.org, (2018).
[24] J. Gullberg, P. Jonsson, A. Nordström, M. Sjöström, T. Moritz, Design of experiments: an efficient strategy to identify factors influencing extraction and derivatization of *Arabidopsis thaliana* samples in metabolomic studies with gas chromatography/mass spectrometry, Anal. Biochem. 331 (2004) 283–295.
[25] J. Xia, I. Sinelnikov, B. Han, D.S. Wishart, MetaboAnalyst 3.0–making metabolomics more meaningful, Nucleic Acids Res. 43 (2015) W251–W257.
[26] S.M. Ellis, H.S. Steyn, Practical significance (effect sizes) versus or in combination with statistical significance (p–values), Manag. Dyn. 12 (2003) 51–53.
[27] L.W. Sumner, A. Amberg, D. Barrett, M.H. Beale, R. Beger, C.A. Daykin, T.W.M. Fan, O. Fiehn, R. Goodacre, J.L. Griffin, T. Hankemeier, N. Hardy, J. Harnly, R. Higashi, J. Kopka, A.N. Lane, J.C. Lindon, P. Marriott, A.W. Nicholls, M.D. Reily, J.J. Thaden, M.R. Viant, Proposed minimum reporting standards for chemical analysis chemical analysis working group (CAWG) metabolomics standards initiative (MSI), Metabolomics 3 (2007) 211–221.
[28] E.L. Schymanski, J. Jeon, R. Gulde, K. Fenner, M. Ruff, H.P. Singer, J. Hollender, Identifying small molecules via high resolution mass spectrometry: communicating confidence, Environ. Sci. Technol. 48 (2014) 2097–2098.
[29] M.T. Alam, G.R. Manjeri, R.J. Rodenburg, J.A.M. Smeitink, R.A. Notebaart, M. Huynen, P.H.G.M. Willems, W.J.H. Koopman, Skeletal muscle mitochondria of NDUFS4$^{-/-}$ mice display normal maximal pyruvate oxidation and ATP production, Biochim. Biophys. Acta Bioenerg. 1847 (2015) 526–533.
[30] F. Valsecchi, C. Monge, M. Forkink, A.J.C. de Groof, G. Benard, R. Rossignol, H.G. Swarts, S.E. van Emst-De Vries, R.J. Rodenburg, M.A. Calvaruso, L.G.J. Nijtmans, B. Heeman, P. Roestenberg, B. Wieringa, J.A.M. Smeitink, W.J.H. Koopman, P.H.G.M. Willems, Metabolic consequences of NDUFS4 gene deletion in immortalized mouse embryonic fibroblasts, Biochim. Biophys. Acta Bioenerg. 1817 (2012) 1925–1936.
[31] R. de Haas, D. Das, A. Garanto, H.G. Renkema, R. Greupink, P. van den Broek, J. Pertijs, R.W.J. Collin, P. Willems, J. Beyrath, A. Heerschap, F.G. Russel, J.A. Smeitink, Therapeutic effects of the mitochondrial ROS–redox modulator KH176 in a mammalian model of Leigh disease, Sci. Rep. 7 (2017) 11733.
[32] D.W. Leong, J.C. Komen, C.A. Hewitt, E. Arnaud, M. McKenzie, B. Phipson, M. Bahlo, A. Laskowski, S.A. Kinkel, G.M. Davey, W.R. Heath, A.K. Voss, R.P. Zahedi, J.J. Pitt, R. Chrast, A. Sickmann, M.T. Ryan, G.K. Smyth, D.R. Thorburn, H.S. Scott, Proteomic and metabolomic analyses of mitochondrial complex I-deficient mouse model generated by spontaneous B2 short interspersed nuclear element (SINE) insertion into NADH dehydrogenase (ubiquinone) Fe-S protein 4 (Ndufs4) gene, J. Biol. Chem. 287 (2012) 20652–20663.
[33] S.M.S. Budde, L.P.W.J. van den Heuvel, R.J.P. Smeets, D. Skladal, J.A. Mayr, C. Boelen, V. Petruzzella, S. Papa, J.A.M. Smeitink, Clinical heterogeneity in patients with mutations in the NDUFS4 gene of mitochondrial complex I, J. Inherit. Metab. Dis. 26 (2003) 813–815.
[34] C. Ugalde, R.J.R.J. Janssen, L.P. van den Heuvel, J.A.M. Smeitink, L.G.J. Nijtmans, Differences in assembly or stability of complex I and other mitochondrial OXPHOS complexes in inherited complex I deficiency, Hum. Mol. Genet. 13 (2004) 659–667.
[35] S.M.S. Budde, L.P.W.J. van den Heuvel, A.J. Janssen, R.J.P. Smeets, C.A.F. Buskens, L. Demeirleir, R. Van Coster, M. Baethmann, T. Voit, J.M.F. Trijbels, J.A.M. Smeitink, Combined enzymatic complex I and III deficiency associated with mutations in the nuclear encoded NDUFS4 gene, Biochem. Biophys. Res. Commun. 275 (2000) 63–68.
[36] M.E. Breuer, P.H.G.M. Willems, J.A.M. Smeitink, W.J.H. Koopman, M. Nooteboom, Cellular and animal models for mitochondrial complex I deficiency: a focus on the NDUFS4 subunit, IUBMB Life 65 (2013) 202–208.
[37] K. Esterhuizen, F.H. van der Westhuizen, R. Louw, Metabolomics of mitochondrial disease, Mitochondrion 35 (2017) 97–110.
[38] A.E. McDonald, N. Pichaud, C.-A. Darveau, "Alternative" fuels contributing to mitochondrial electron transport: importance of non-classical pathways in the

diversity of animal metabolism, Comp. Biochem. Physiol. B 224 (2018) 185–194.
[39] N.J. Watmough, F.E. Frerman, The electron transfer flavoprotein: ubiquinone oxidoreductases, Biochim. Biophys. Acta Bioenerg. 1797 (2010) 1910–1916.
[40] A.P. Russell, L. Ghobrial, C.R. Wright, S. Lamon, E.L. Brown, M. Kon, M.R. Skelton, R.J. Snow, Creatine transporter (SLC6A8) knockout mice display an increased capacity for in vitro creatine biosynthesis in skeletal muscle, Front. Physiol. 5 (2014) 314.
[41] J.G. Bogner-Strauss, *N*–Acetylaspartate metabolism outside the brain: lipogenesis, histone acetylation, and cancer, Front. Endocrinol. 8 (2017) 240.
[42] J. Phang, Proline metabolism in cell regulation and cancer biology: recent advances and hypotheses, Antioxid. Redox Signal. (2017), https://doi.org/10.1089/ars.2017.7350.
[43] G. Wu, F.W. Bazer, R.C. Burghardt, G.A. Johnson, S.W. Kim, D.A. Knabe, P. Li, X. Li, J.R. McKnight, M.C. Satterfield, T.E. Spencer, Proline and hydroxyproline metabolism: implications for animal and human nutrition, Amino Acids 40 (2011) 1053–1063.
[44] G.A. Qureshi, A. Gutierrez, J. Bergström, Determination of histidine, 1-methylhistidine and 3-methylhistidine in biological samples by high-performance liquid chromatography: clinical application of urinary 3-methylhistidine in evaluating the muscle protein breakdown in uraemic patients, J. Chromatogr. B Biomed. Sci. Appl. 374 (1986) 363–369.